Zeitschrift: Bulletin der Schweizerischen Akademie der Medizinischen Wissenschaften = Bulletin de l'Académie suisse des sciences médicales = Bollettino dell' Accademia svizzera delle scienze mediche

Herausgeber: Schweizerische Akademie der Medizinischen Wissenschaften

Band: 31 (1975)

Artikel: Simulation of pathologic electrocardiograms : the role of Durrer layers in the normal, the hypertrophied and the ischemic heart

Autor: Rosenberg, R.M.

DOI: https://doi.org/10.5169/seals-308003

Bull. schweiz. Akad. med. Wiss. *31*, 79–99 (1975)

University of California, Berkeley, California, U.S.A.

Simulation of Pathologic Electrocardiograms: The Role of Durrer Layers in the Normal, the Hypertrophied and the Ischemic Heart

R. M. Rosenberg

Introduction

Recently, a computer model of electrical cardiac activity was described which generates high fidelity 12-lead electrocardiograms (ECG's) of a normal heart of intermediate (45 degree) orientation [1]. Briefly, this model consists of eleven myocardial components; two of them represent the atria, and the other nine model the ventricles and the septum. Each of these components is represented by a dipole of known and fixed location and direction, and of variable strength. The location is determined by the location of the centroid of the component, and the direction is that of signal propagation at the location in question. Here, "direction of signal propagation at a location" is understood to mean the direction normal to the wave front of the depolarization wave at the location in question, pointing in the direction of wave front advance. The strength of the dipole as a function of time is modeled on the resultant dipole or, in effect, the diphasic action potential which is generated by a single myocardial cell as the transmembrane action potential (TMAP) spreads over the cell surface. The reason for choosing the cell as a model of the electrical behavior of a myocardial component is that, as regards electrical activity, "the heart muscle behaves in many ways as if it were a single cell" [2]. For instance, the diphasic action potential resulting from the signal spread over the myocardial cell surface resembles in great detail that observed during the activation of a myocardial strip. The onset of activation of each of the eleven dipoles is determined from the experimental results regarding the spread of depolarization through the heart found by DURRER et al. [3] and SCHER [4].

Models of the type described here are of the "distributed dipole type", and they are not new. Their list is too long to refer to all of them here. However, we wish to mention the highly successful models of SELVESTER and his group [5–8] which have been utilized not only to model normal electrical heart activity but also infarction [7, 8] and hypertrophy [5]. A direct comparison of

SELVESTER's results with ours is difficult because he and his group have been concerned with ventricular depolarization and modeling the QRS-complex while our interest has been centered on repolarization and the S-T,T effects as well.

Our model reproduces the T-wave polarity seen in clinical ECG's, and our explanation of the T-wave genesis is based on the experimental observations of the ventricular recovery sequence reported by VAN DAM and DURRER [9]. They found in an important experimental study some fifteen years ago that the recovery of excitability in the left ventricular wall was more advanced in the middle layers than in the endocardial layers, and somewhat more advanced than in the epicardial layers; we have called these the "Durrer layers" [1]. The findings of VAN DAM and DURRER were largely confirmed by BURGESS et al. [10] in a relatively recent study of the recovery sequence in the dog heart. The mechanism of the unexpected T-wave polarity rests on the so-called "contiguity effect" produced by the interface between adjacent or contiguous Durrer layers.

Two cells belonging to different Durrer layers have by definition different TMAP-durations. If these cells are *contiguous*, the difference in TMAP-duration gives rise to a dipole which would be absent if the two cells were not contiguous. This new dipole has been called by us the contiguity effect [1]; it is this contiguity effect which produces the concordance of R and T-waves.

This explanation of the T-wave polarity is not new; it was already anticipated some 40 years ago by WILSON et al. [11] in an admirable paper, it was suggested by VAN DAM and DURRER in their experimental study [9] and it was explained that way in a series of papers associated with the names of BURGESS, HARUMI and ABILDSKOV [12, 13] and summarized by BURGESS in 1972 [14].

It turns out that the contiguity effect of contiguous cells having different TMAP's not only explains the T-wave polarity, but it also furnishes a mechanism for the ECG-manifestations of left ventricular hypertrophy (LVH) and acute ischemia [15].

Methods and Results

The Myocardial Cell

In order to compute the resultant dipole which arises from the spread of depolarization and repolarization over the cell membrane, it is necessary to give a mathematical representation of the cell geometry and of the TMAP.

For the purpose of this study, the cell is assumed to be spherical. That choice is not a literal image of a myocardial cell which is elongated and is shaped more nearly like a cylinder, but it turns out that for the analysis of *electrical* cardiac activity, the sphere is the best choice. From the studies of DURRER et al. [3] and SCHER [4], it is seen that the direction of signal propagation does not generally proceed in the direction of the longitudinal axis of the

cell; in the left ventricular wall the direction of signal propagation is more nearly normal to that axis, and in the right ventricular wall in some locations it is neither normal to, nor along, that axis. But, if the direction of signal propagation in the heart bears no evident relation to the cell orientation, one must choose for the model of electrical cell activity a shape which has no preferred direction; the only such shape is the sphere.

The functional representation of the TMAP has been chosen so as to resemble that of non-pacemaker cells because these are known to be the major contributors to the ECG. Its mathematical formulation is

$$\left.\begin{aligned} f(t) &\equiv o && \text{in } o<t<t_o\,, \\ f(t) &\equiv k && \text{in } t_o<t<t_o+p\,, \\ f(t) &= k\left[1-\frac{2(t-t_o-p)^2}{w^2}\right] && \text{in } t_o+p<t<t_o+p+\frac{w}{2}\,, \\ f(t) &= \frac{2k(t_o+p+w-t)^2}{w^2} && \text{in } t_o+p+\frac{w}{2}<t<t_o+p+w\,, \end{aligned}\right\} \quad (1)$$

where k is an amplitude constant in millivolts, p and w are the duration of the depolarized state and the repolarization time in milliseconds, respectively, and t_o is the instant of onset of depolarization. Typically, $k = 100$ mv, $p = 70$ msec, $w = 100$ msec. The graph of this TMAP is shown in Fig. 1.

For a signal propagation speed u in the myocardium, the average speed of propagation over the cell surface is easily shown to be [1]

$$\eta = \frac{1}{2}\pi u \quad (2)$$

and the diphasic action potential generated from the signal spread over the cell surface of a spherical cell of radius r has been shown [1] to be

$$D(t) = \pi r^2 \int_o^{\pi} \sin 2\beta\, f\left(t-t_o-\frac{\beta r}{\eta}\right)\, d\beta \quad (3)$$

where f is defined in (1). This is the strength of the dipole of a single cell, and its graph is shown in Fig. 2. It is seen that this curve consists of a sharply peaked positive wave which we call a QRS-wave in analogy to the clinical ECG, a horizontal portion of zero potential which we call an S-T segment, and a broad wave of negative polarity which we call a T-wave.

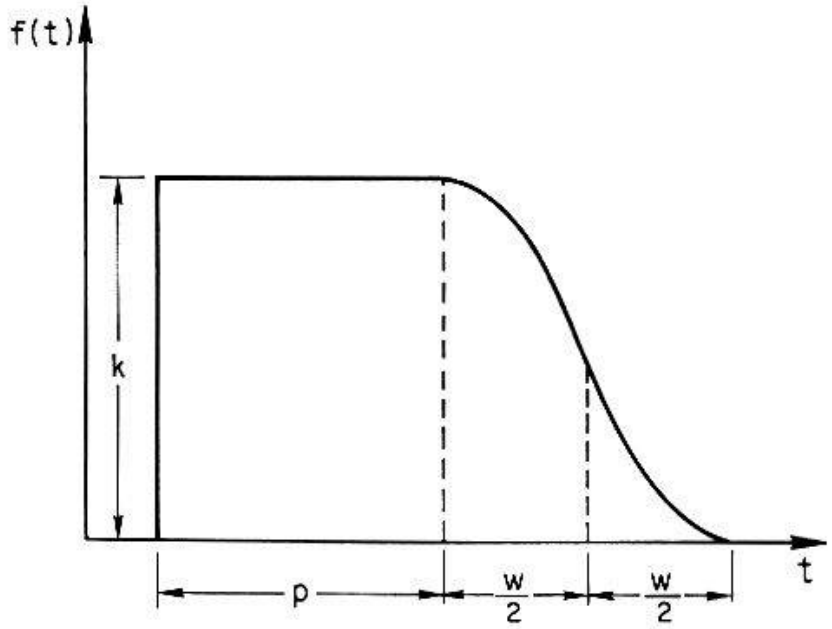

Fig. 1. Graph of mathematical representation of transmembrane action potential of non-pacemaker cell.

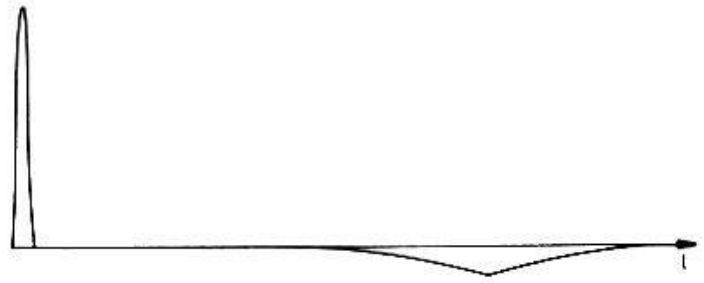

Fig. 2. Diphasic action potential of spherical cell.

The important result to be deduced from (3) is that the diphasic action potential amplitude is for all time proportional to the square of the cell radius, and one can easily show that the QRS-duration is linearly proportional to the cell radius [16].

In analogy to the ECG, we call the algebraic sum of the area under the diphasic curve of Fig. 2 the "cell gradient", or the cell gradient is defined as

$$G = \int_{t_o}^{T} D(z)\, dz \tag{4}$$

where T-t_o is the interval from onset of depolarization at the first point on the cell to termination of repolarization at the last point on the cell. It can be shown that the cell gradient defined in (4) is zero. WILSON et al. [11] have given a demonstration of this result for a one-dimensional muscle strip by a

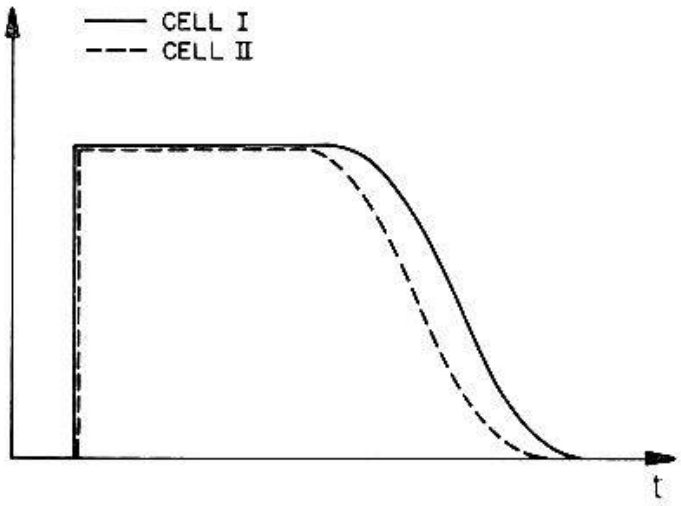

Fig. 3. Transmembrane potentials of two cells with different action potential durations.

geometrical argument, and a strict mathematical proof for a three-dimensional cell has been given earlier [1].

The Contiguity Effect in Two Cells

Consider two contiguous cells such that the line connecting their centers lies in the direction of signal propagation, and let them have different TMAP's.

To fix ideas, let the signal propagate from Cell I to Cell II, and let Cell I belong to the endocardial Durrer layer and Cell II to the intermediate Durrer layer. Thus, the point of contact B between the two cells is a point on the interface between adjacent Durrer layers. Let the spread of activation begin at point A of Cell I diametrically opposite the contact point B, let it proceed over the surface of Cell I to point B and then continue from point B on Cell II to point C which is diametrically opposite point B. Then, the activation of point B on Cell I begins simultaneously with that of point B on Cell II, and the two action potentials at B look as shown in Fig. 3. It is seen that the TMAP-duration of Cell II is shorter than that of Cell I because they belong to different Durrer layers. Therefore, there exists a potential difference between neighboring points on Cell I and Cell II which begins at the instant when Cell II begins to repolarize, and which ends when the repolarization of Cell I is completed. Such a potential difference between neighboring points can be modeled by a dipole which, in this example, makes a positive contribution to the diphasic curve of the two cells because the voltage difference is positive, i.e., it coincides with the direction of signal propagation. If the TMAP-duration in Cell II had been longer (rather than shorter) than that in Cell I, the contribution of the contiguity effect would have been negative. The resultant diphasic curve of the two cells is shown in Fig. 4. It is seen that, for the example considered here, the contiguity effect has reversed the polarity of the resultant T-wave.

If one considers the cell gradient of the two cells as the sum of the gradients of each, the two-cell gradient would have been zero in the absence of the

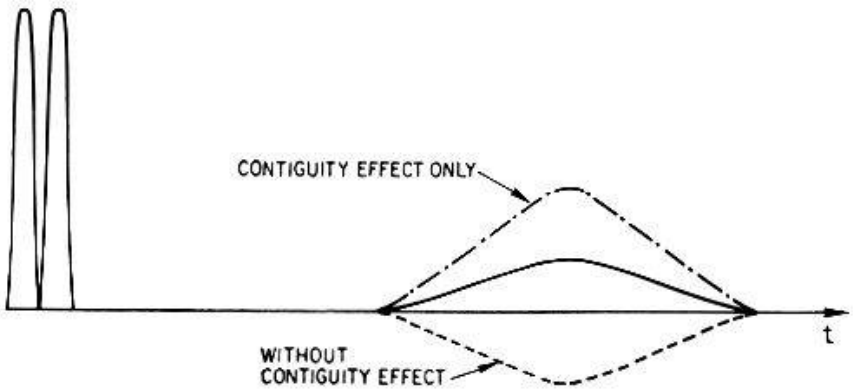

Fig. 4. Resultant diphasic action potential of two contiguous cells having transmembrane potentials of different duration.

contiguity effect, or the area under the two sharp peaks at the left of Fig. 4 would be the same as that under the dotted curve labelled "No contiguity effect". However, in the presence of the contiguity effect the two-cell gradient is positive.

The Heart Model

The heart model used in this study has been described elsewhere [1]. It consists of eleven components; two of these are the atria and nine more represent the ventricular septum and the ventricles in the manner shown in Fig. 5. The decomposition of the left ventricle is shown schematically in greater detail in Fig. 6. The septum and the left ventricle are composed of contiguous Durrer layers with boundaries normal to the direction of signal propagation. Every component without Durrer layers, and every Durrer layer, is in turn decomposed in the model into electrically homogeneous sublayers whose boundaries are also normal to the direction of signal propagation. In this way, it is possible to follow the progress of the depolarization and repolarization waves through the component, or through the Durrer layer, and it is also possible to introduce local malfunctions in pre-assigned portions of every component, or of every Durrer layer.

In our model of electrical heart activity, the location and direction of a number of dipoles must be defined. In general, the dipole location is identified with that of the centroid of the myocardial tissue represented by the dipole, and the dipole direction with that of signal propagation at the location in question. Location and direction are given relative to a coordinate system with origin at the centroid of the heart. In conformity with normal practice in cardiology, the frontal plane is the xy-plane with x-axis positive right-to-left and y-axis positive head-to-foot. The sagittal plane is the y, z-plane with z-axis positive in the anteroposterior direction.

Each sublayer is represented by a dipole whose strength as a function of time is given by a diphasic curve resembling in shape that of a single cell (see

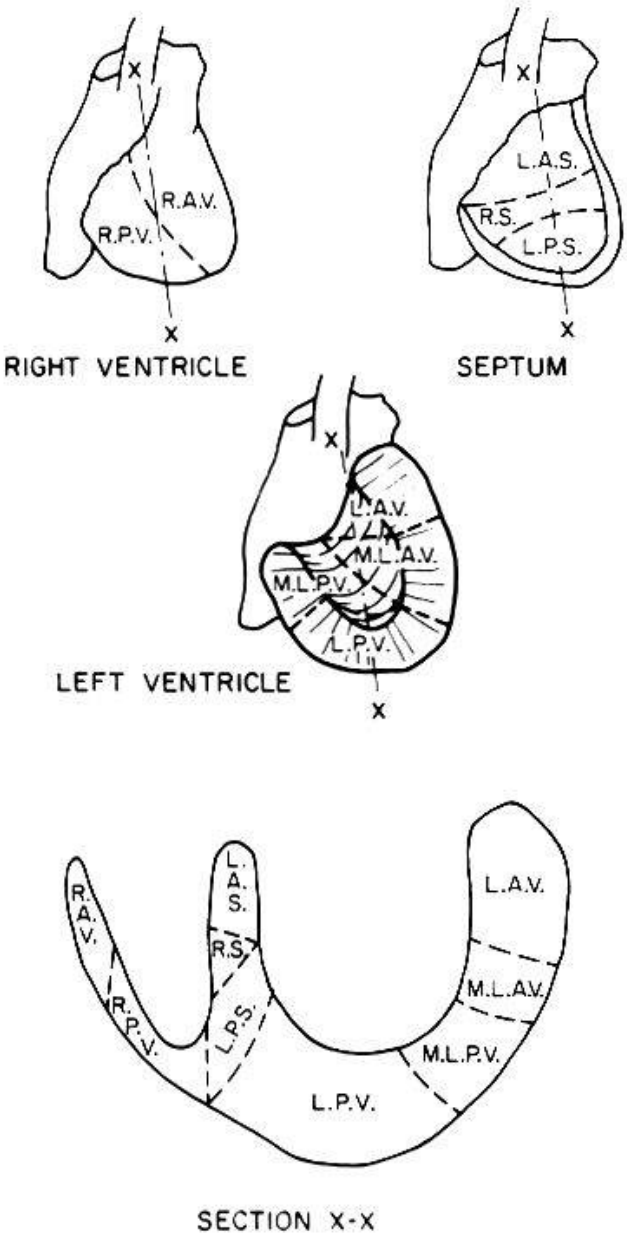

Fig. 5. Decomposition of ventricles and septum into components. R.A.V. = right anterior ventricle; R.P.V. = right posterior ventricle; L.A.S. = left anterior septum; R.S. = right septum; L.P.S. = left posterior septum; L.A.V. = left anterior ventricle; M.L.P.V. = middle left posterior ventricle; L.P.V. = left posterior ventricle.

Fig. 2), but with amplitude proportional to the volume of the sublayer; i.e., proportional to the number of normal size myocardial cells in it. The dipole of the component is the sum of the sublayer dipoles, each displaced with respect to its neighbor in accordance with the signal propagation velocity. The activation of the diphasic action potential of each component occurs at the arrival time of the depolarization wave at the component represented by that dipole. The data regarding the progress of the depolarization wave through the human heart utilized by us were obtained in a delicate series of observations by DURRER et al. [3].

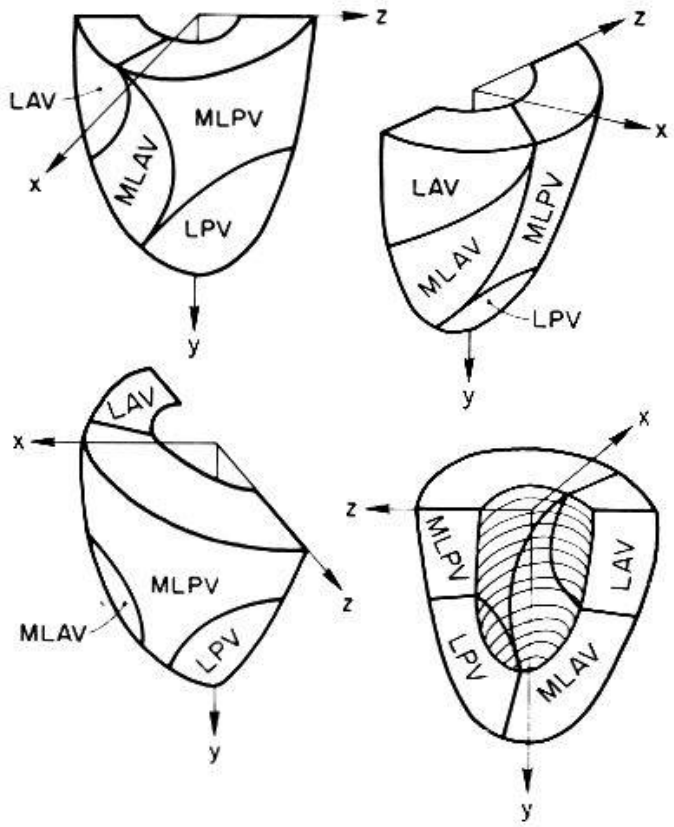

Fig. 6. Details of decomposition of left ventricle.

The Skin Surface Potentials [*1*]

The twelve leads of a standard ECG are obtained from the skin surface potentials at nine points on the body; these potentials are induced by the dipoles which model the heart. As the body is a volume conductor whose boundaries and local conduction properties can be determined by measurement, it is possible, in principle at least, to compute the skin surface potentials at given points on the conductor boundary, induced by dipoles of known location, direction and moment. However, the required properties of the body are difficult to ascertain and once known, the computation of the skin surface potentials leads to an elaborate and computationally difficult boundary value problem. GELERNTER and SWIHART [16] have examined the problem of the boundedness of the volume conductor, SELVESTER and his group have taken into account boundary and distance effects [6, 7] and inhomogeneity within the body [7], a critical study of this problem has been made by SCHER et al. [17], and important contributions to the effect of volume conductor inhomogeneity have been made by GESELOWITZ [18, 19] in his studies of electrical and magnetic fields generated by dipoles in inhomogeneous, bounded volume conductors.

The difficulties just alluded to disappear when the body is regarded as a portion of a homogeneous volume conductor of infinite extent. Partly to keep the problem computationally tractable, but mostly because the problems treated by us are present regardless of the detail properties of the volume

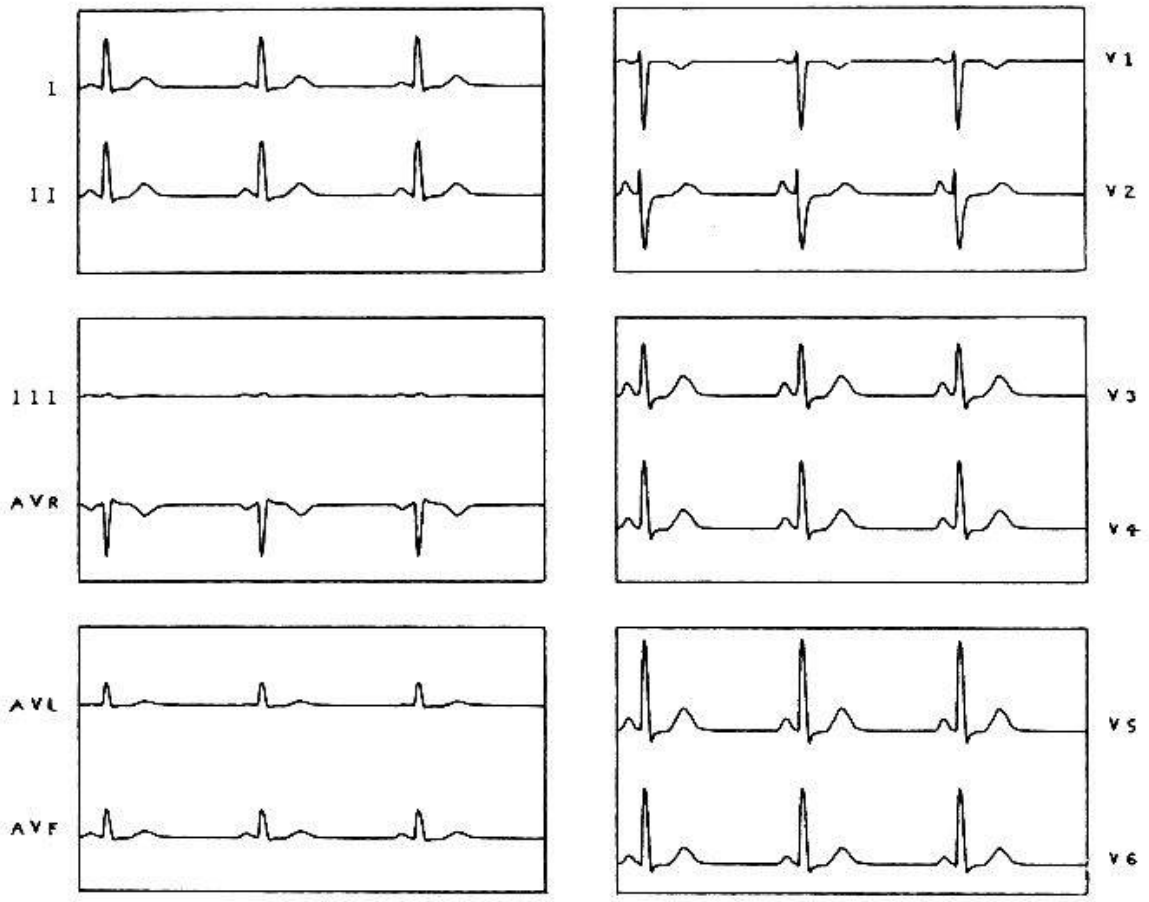

Fig. 7. Computer-generated 12-lead ECG of normal heart of intermediate (45 degree) orientation.

conductor, we postulate the existence of an "equivalent, electrically homogeneous body" immersed in an infinite, electrically homogeneous medium having the same coefficient of conductivity as the equivalent body. Equivalence is established when the skin surface potentials at the nine points on the body, induced by the same dipole, are equal in the actual and the equivalent body.

In computing the skin surface potentials we use the classical, quasi-static approximation; i.e., while the electrical sources in the heart are considered as time-varying, one may calculate the induced potentials as though steady state conditions existed at every instant.

The 12-lead computer-generated ECG's of a normal heart of intermediate (45 degree) orientation are shown in Fig. 7. It is seen that they resemble clinical ECG's in great detail.

A computer model is particularly suitable for demonstrating the contiguity effect of adjacent Durrer layers on the polarity of the T-wave because, in such a model, one can simply delete that contiguity effect. In Fig. 8 the twelve leads of the ECG *without* the contiguity effect of adjacent Durrer layers are shown. It should be realized that in that computation the Durrer layers were retained; only the effect of their interfaces was suppressed. As a result, all leads have zero ventricular gradient.

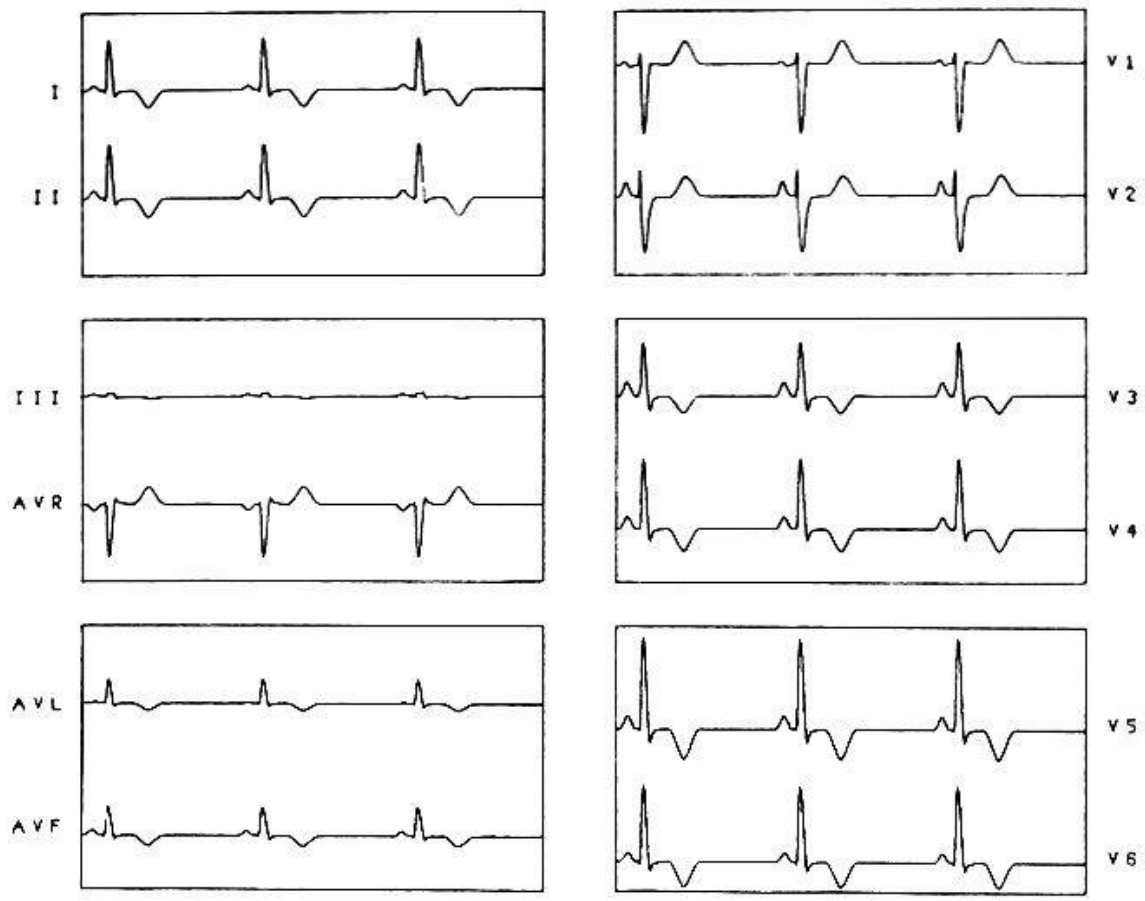

Fig. 8. Computer-generated 12-lead ECG of normal heart with contiguity effect of adjacent Durrer layers suppressed.

In comparing Figs. 7 and 8, it is seen that the contiguity effect reverses the T-wave polarity in all leads except V_2. In that lead, the T-wave is actually more positive without than with the contiguity effect although the difference is not large. It may be concluded that, for the heart orientation considered here, the ventricular gradient in V_2 normally is nearly zero. As V_2 is the only lead with electrode position in the sagittal plane, it is implied thereby that the dipoles of components having Durrer layers lie nearly in the frontal plane.

Left Ventricular Hypertrophy [*15*]

The microscopic evidence of myocardial hypertrophy appears to be an increase in the size of the muscle fibers but no increase in their number [20, 21], and UHLEY has shown [22] that the TMAP of hypertrophied cells remains normal.

Now, the contiguity effect of adjacent Durrer layers depends only on the differences in TMAP between contiguous cells belonging to different layers, and on the total number of contacts between such unlike cells. Therefore, the contiguity effect of adjacent Durrer layers remains unchanged in hypertrophy because the number of cells and the TMAP's remain unchanged. Hence, hyper-

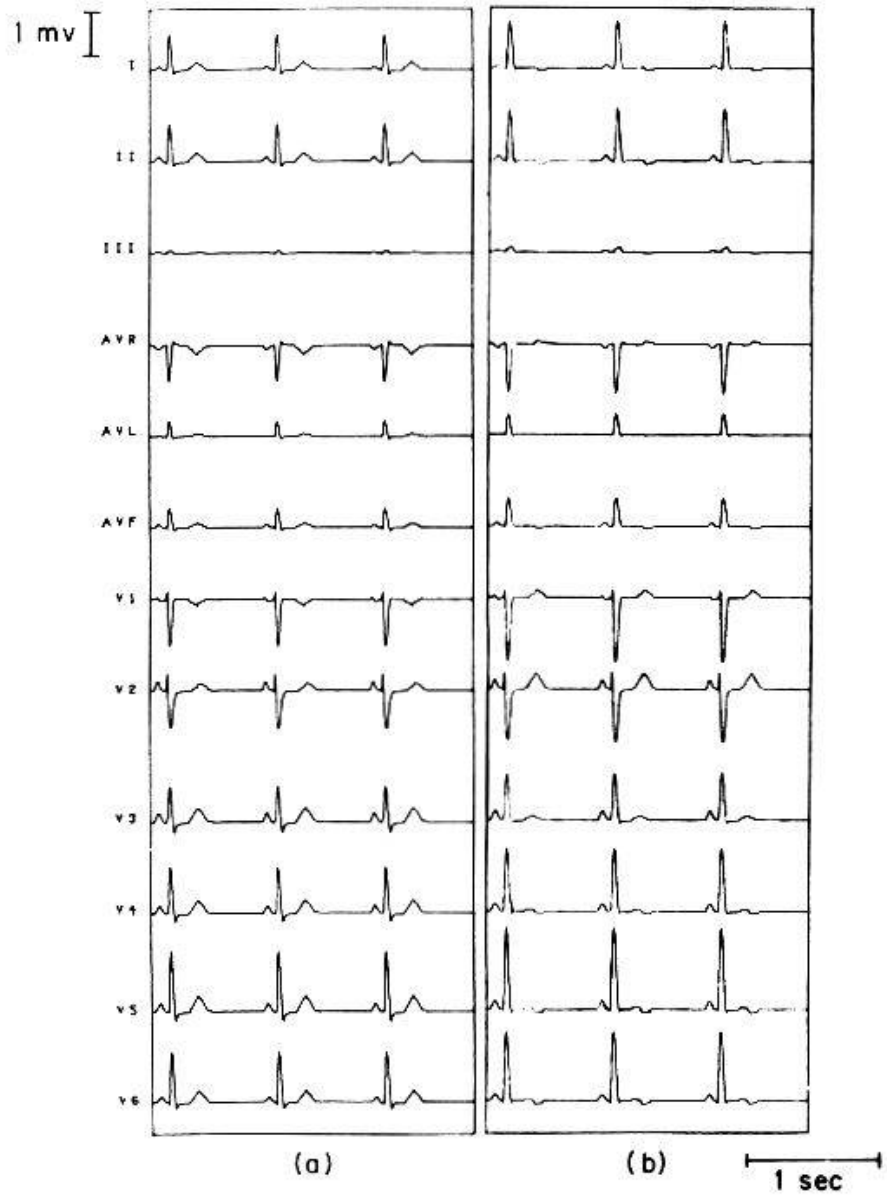

Fig. 9. Computer-generated ECG's; (a) normal; (b) left ventricular hypertrophy.

trophy is modeled by increasing the cell radius of the affected component and by leaving the contiguity effect of adjacent Durrer layers unchanged.

The example of left ventricular hypertrophy considered here is hypertrophy of the entire left ventricle produced by an increase in cell radius of 15 per cent; this produces a volume increase of 52 per cent of the left ventricular myocardium. No heart rotation due to hypertrophy is included in the example.

The computer-generated 12-lead ECG's for this example are shown next to the normal ECG's in Fig. 9. In general, they show an R-wave amplitude increase of 36 per cent except in V_1 and V_2 where deep S-waves are seen. In addition, the ventricular activation time (VAT) is increased in the average of the 12 leads by approximately 14 per cent; moreover, the T-wave is either flattened or inverted. These configurations correspond to clinical experience [23].

Our computer results are not unexpected. It was observed in connection with (3) that the diphasic action potential amplitude is proportional to the square of the cell radius, and the QRS-duration varies directly as that radius. Thus, one would expect a VAT-increase on the order of 15 per cent, and an R-wave increase of 32.5 per cent. The slight variation of the computer output from these predictions comes about because R-wave amplitude and QRS-duration are not produced by the left ventricle only, but by both ventricles.

The T-wave distortion comes about because of the unchanged contiguity effect. In the absence of this effect the ventricular gradient is zero; hence, an R-wave increase of 36 per cent would bring with it a negative T-wave whose amplitude is also increased by 36 per cent. Hence, the negativity of the T-wave is increased, but the erecting effect of the Durrer layers is unchanged. Thus, one may well expect flattened or inverted T-waves in left ventricular hypertrophy.

In the literature the increased R-wave is frequently regarded as puzzling in view of the unchanged TMAP, and the T-wave distortion is ascribed to unknown repolarization changes [23]. However, these manifestations are easily explained by the mechanism presented here, thereby lending further support to the explanation of the upright T-wave from the contiguity effect of adjacent Durrer layers.

Acute Ischemia [15]

With respect to ischemic lesions there exists a good deal of experimental evidence [24, 25] to show that acute ischemia reduces the amplitude of the transmembrane action potential; i.e., the voltage spread between the plateau (or the depolarized state) and the resting potential. This is brought about both by an increase in the resting potential and by a decrease of the potential in the depolarized state [24].

Hence, if one considers two contiguous cells, Cell I and Cell II, such that the direction of signal propagation is from Cell I to Cell II, and Cell I is normal while Cell II is ischemic, the TMAP's of these two cells at their contact points look as shown in Fig. 10 where the solid curve is that of Cell I. From this figure it is seen that, now, there exists a potential difference between two neighboring points, one in Cell I and the other in Cell II, during the entire TMAP-duration, and, therefore, there exists a contiguity effect during this entire interval. This has the effect of raising the S-T segment of the two-cell diphasic action potential as shown in Fig. 11. If Cell I were ischemic and Cell II normal, the S-T segment would have been depressed.

The cases of acute ischemia considered here are high anterior, and inferior posterior acute ischemia of the left ventricle. The high anterior ischemia affects all of LAV and approximately 25 per cent of MLAV, and the inferior posterior ischemia affects LPV (see Fig. 5). The areas involved are the shaded areas shown schematically in Fig. 12.

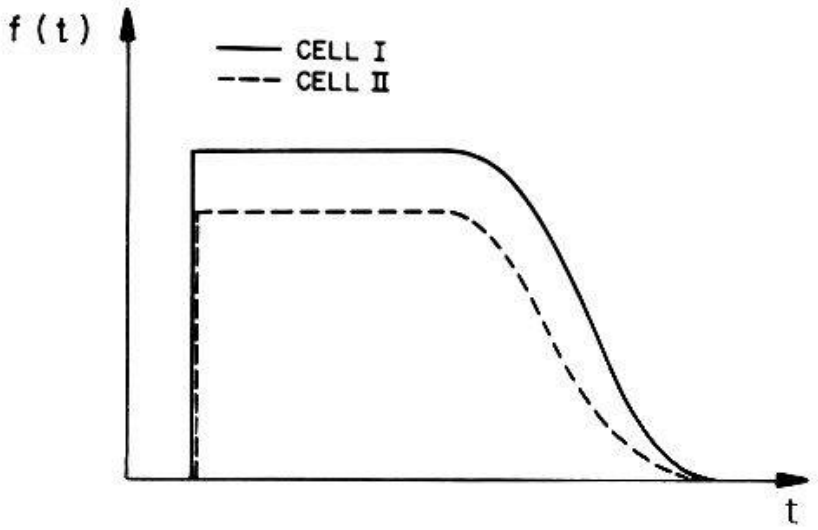

Fig. 10. Model of transmembrane action potential of normal Cell I and ischemic Cell II.

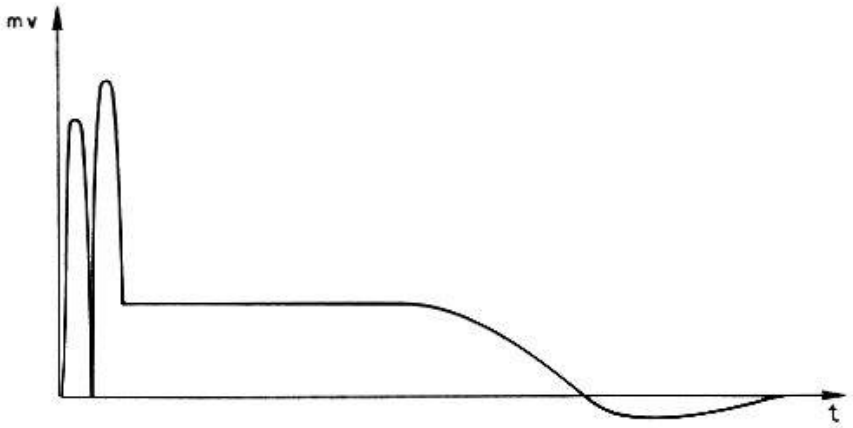

Fig. 11. Resultant diphasic action potential of two contiguous cells one of which is ischemic.

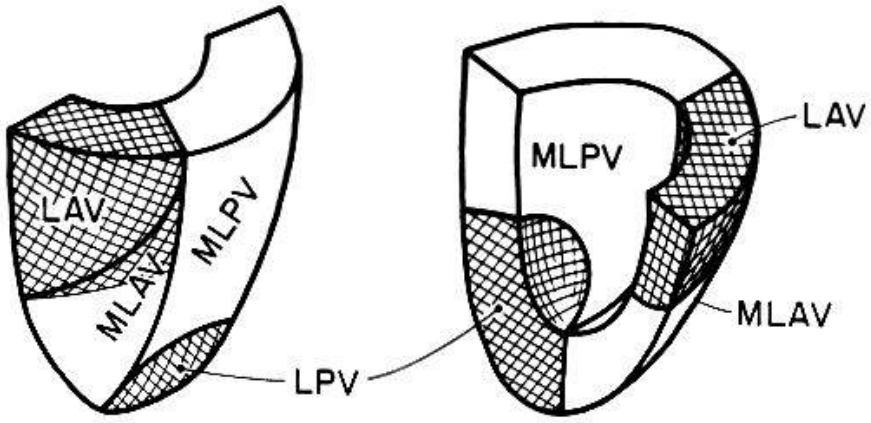

Fig. 12. Areas of left ventricle involved in acute ischemia; ischemic areas shown shaded.

We model only subendocardial and epicardial ischemia; transmural lesions have not been considered. The component of the ventricular wall affected by ischemia has been divided into an epicardial and subendocardial layer as shown

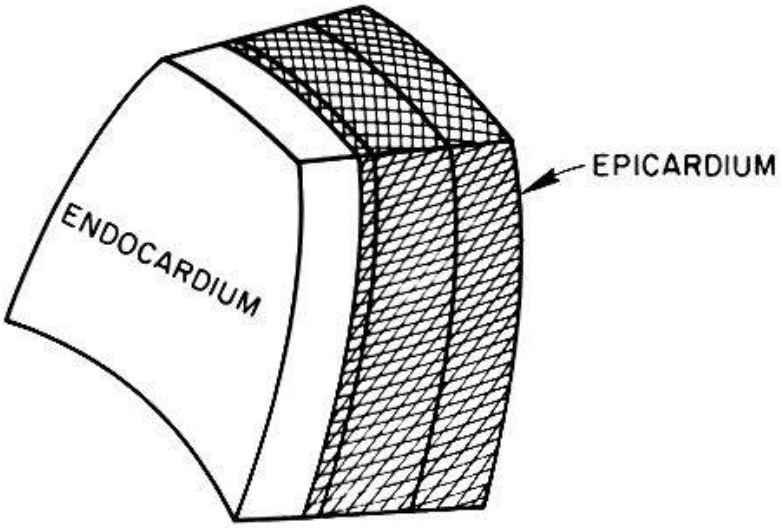

Fig. 13. Separation of ventricular wall into epicardial tissue (shaded) and subendocardial tissue (not shaded).

in Fig. 13. The epicardial portion comprises the epicardial and intermediate Durrer layer and one sublayer of the endocardial Durrer layer; this is the shaded portion of Fig. 13. The endocardial portion includes the remainder of the ventricular wall and is shown as the unshaded portion of Fig. 13.

The computer-generated 12-lead ECG's of high anterior ischemia are shown in Fig. 14, and those of inferior posterior ischemia are shown in Fig. 15. In each illustration the first column gives the normal ECG for easy comparison, the second shows subendocardial ischemia, and the third epicardial ischemia.

A broad summary of our theoretical study coincides completely with the general conclusions reached by PRINZMETAL et al. in an experimental study of 89 experiments on 34 dogs [24]: There exists a quantitative linear relationship between surface and intracellular electrograms, and S-T segment displacement in ECG's is among the most significant changes produced by acute myocardial ischemia.

As a general observation, it is seen from Figs. 14 and 15 that, where subendocardial and epicardial ischemia is considered in the same part of the ventricle, the S-T segment displacements in these two cases are in opposite directions. This is expected because the contiguity effect for signal propagation from normal to ischemic cells is opposite to that from ischemic to normal cells; the former occurs in epicardial ischemia, the latter in subendocardial ischemia.

Similarly, the S-T segment shifts due to posterior ischemia are generally in opposite directions to those of anterior ischemia when lesions in the same layers are compared. Again, this is expected because the dipoles of the affected components point approximately in opposite directions in these two cases.

Both results coincide with clinical observations where it is expected that tracings taken directly over the injured areas show S-T segment elevation, but if normal muscle lies between the injured muscle and the electrode, S-T segment

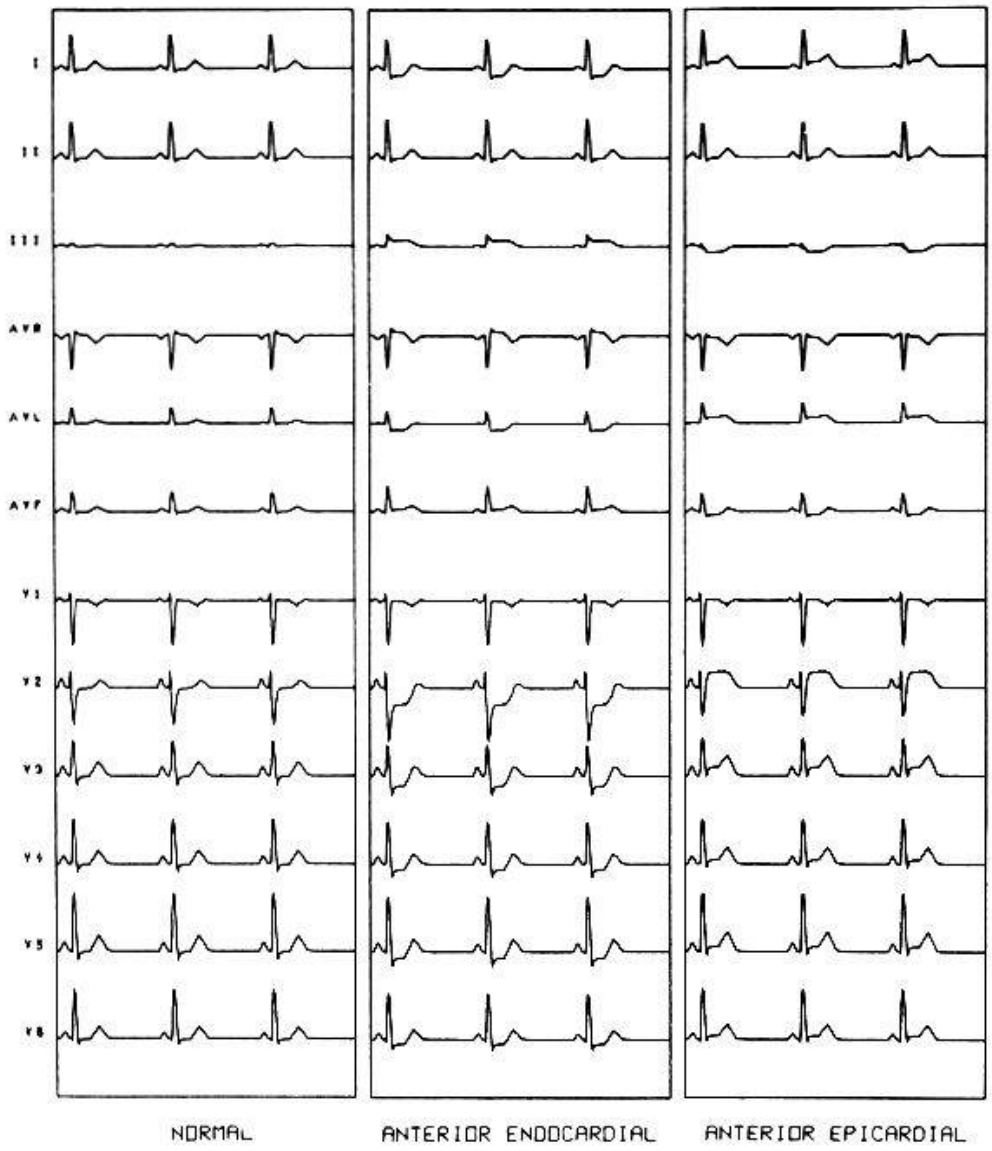

Fig. 14. Two cases of high anterior ischemia.

depressions is expected [23]; while we do not believe that this rule discloses a mechanism, it is certainly true in our example.

It may seem surprising that, in our example, the amount of S-T segment displacement is nearly the same for subendocardial and epicardial ischemia even though twice as much tissue volume is ischemic in the epicardial case than in the subendocardial. To understand the reason for this it must be realized that a dual electrical effect is produced by ischemia: one is a reduction in transmembrane potential amplitude, the other is the contiguity effect produced on the boundary between normal and ischemic tissue. The first effect is proportional to the *volume* of the ischemic tissue, the other is an *area* effect.

Assume that Fig. 13 shows the portion of the ventricular wall that is involved in ischemic changes. Then, it is evident that in the case of epicardial ischemia, slightly more than twice as much myocardial tissue is ischemic than

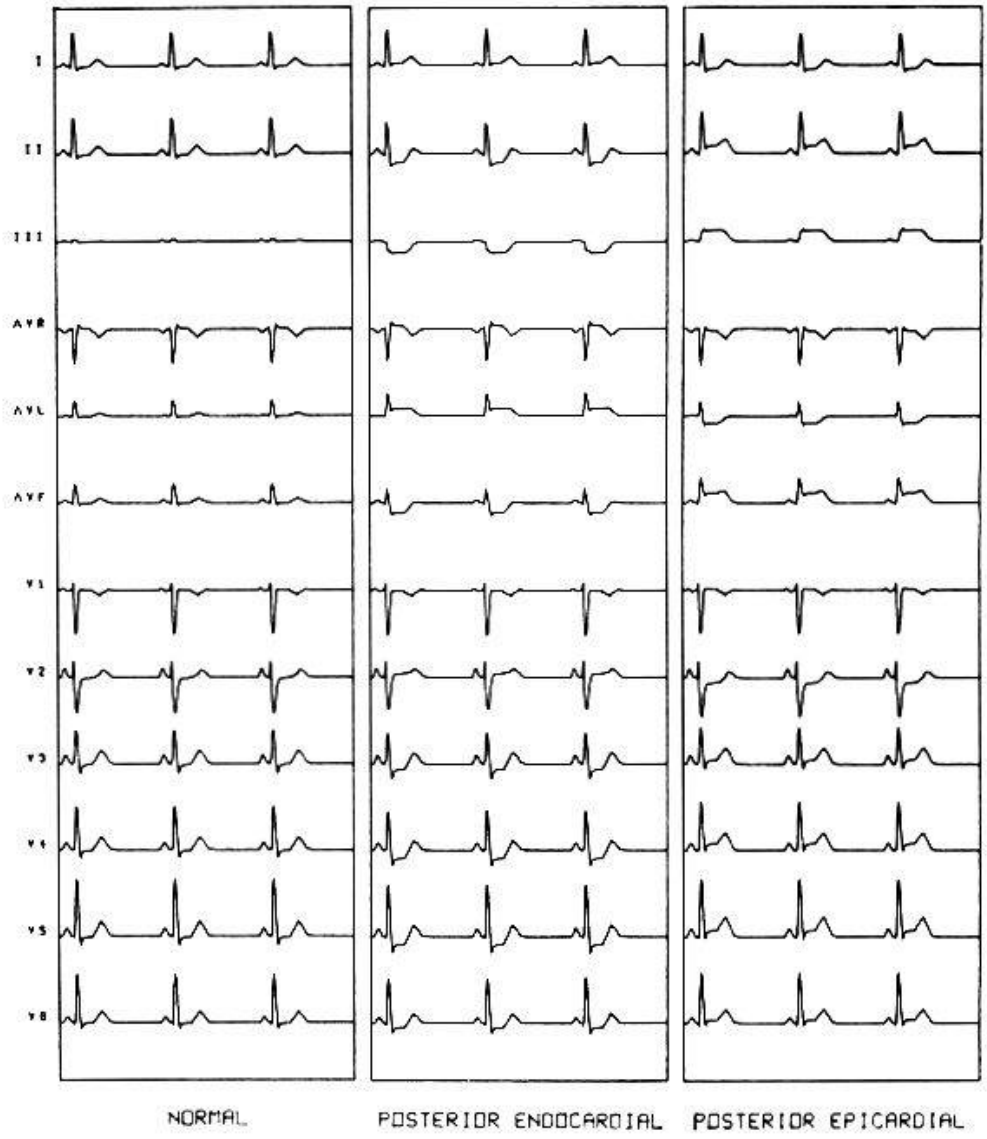

Fig. 15. Two cases of inferior posterior ischemia.

in the subendocardial case. However, the area normal to the conduction path separating normal from ischemic tissue is the same in both cases. Therefore, the S-T segment shift is equal in amount in both cases, although opposite in direction.

The volume effect due to a reduction in electrical activity results in reduced amplitudes in the QRS-complex and the T-wave; however, we will now show that this effect is too small in our example to be readily evident from an examination of the ECG's. In the example, approximately 20 per cent of the ventricular wall is involved in ischemia. In the subendocardial case, one third or approximately 7 per cent of the ventricular myocardium is ischemic, and in the epicardial case, 14 per cent of the ventricular myocardium is ischemic. Hence, only 7 per cent more ventricular tissue is ischemic in the latter case than in the former. Now the reduction in transmembrane potential is 20 per cent in our example. Therefore, the amplitude difference of QRS and T-waves in

these two cases cannot exceed 20 per cent of 7 per cent; i.e., 1.4 per cent. This is too small to be easily seen even though careful measurements show a very small difference.

From a viewpoint of interpretation of ECG data, it is important to realize that the most obvious effect of acute ischemia, the S-T segment shift, is *not* a quantitative measure of the volume of ischemic tissue present, but rather of the cross-sectional area of such tissue normal to the signal flow. Thus, one should not necessarily expect a direct correlation between S-T segment shift and the result of methods of evaluating ischemia which depend on the volume of the ischemic lesion (such as enzyme tests in the case of necrosis). For instance, if the reduction in electrical activity doubles while the ischemic area remains constant, the S-T segment shift also doubles. However, where ischemic lesions in equal locations, and having equal reductions of electrical activity, also involve equal volumes of ischemic tissue but one occupies twice as large an area as the other, that with the larger area will have double the S-T segment shift. Finally, in many cases, an increase in the area of a lesion will involve an equal increase in its volume, and in these cases a direct correlation between S-T segment shift and volume-measuring tests should be readily demonstrable.

It is seen from Figs. 14 and 15 that acute ischemia produces R, S, and T-wave changes in addition to the S-T segment displacement. In general, the peaks of the R-, S- and T-wave are shifted in the same direction as the S-T segment. In the case of the T-wave this would be expected because the reduction of 20 per cent in transmembrane potential occurs during the plateau as well as the repolarization phase, and the latter is responsible for the T-wave formation. In the case of the R- and S-waves the reason is that the QRS-complex formation is not yet completed when the depolarization wave encounters the interface between normal and ischemic tissue; hence the shift produced by the ischemia starts prior to the beginning of the S-T segment formation.

Our computer model has produced a quantitative correspondence between the severity of ischemia on the one hand and ECG response on the other where the term "severity" must be understood to mean diminution of electrical signal output. It appears reasonable to expect that that correspondence could eventually be utilized in diagnosis, for monitoring during treatment, and for other clinical purposes.

Abstract

A mechanism is described which explains the electrocardiographic manifestations of cellular hypertrophy and acute ischemia. This mechanism arises from neighboring cells having different transmembrane action potentials, and it has been called the "contiguity effect". The contiguity effect of adjacent "Durrer layers" (defined in the paper) gives rise to the T-wave distortions in hypertrophy and is also responsible for the polarity of the normal T-wave.

This mechanism has been incorporated in a computer model of electrical heart activity which generates high fidelity 12-lead electrocardiograms. It is shown that the increase in R-wave amplitude and in ventricular activation time, and the flattening and/or polarity reversal of the T-wave in hypertrophy is due to an increase in the size of myocardial cells, and the S-T segment shift in acute ischemia is produced by the contiguity effect between normal and ischemic cells. For a lesion of given size, the S-T segment shift is linearly proportional to the "severity"; i.e., the reduction in electrical activity, of ischemic cells, and for a lesion of given severity, the S-T segment shift is a measure of the area, not the volume, of ischemic tissue. Therefore, a direct correlation does not necessarily exist between volume measuring tests (such as serum enzyme values in the case of necrosis) and S-T segment shifts in acute ischemia.

Zusammenfassung

Es wird ein Mechanismus beschrieben, der die EKG-Bilder der zellulären Hypertrophie und der akuten Ischämie erklärt.

Dieser Mechanismus entsteht aus benachbarten Zellen mit differenten Aktionspotentialen und wird als Grenzflächeneffekt ("contiguity effect") bezeichnet. Dieser Grenzeffekt von benachbarten «Durrerschen Schichten» – die definiert werden – ist Anlass der T-Wellen-Auslenkung bei Hypertrophie und ist auch verantwortlich für die Polarität der normalen T-Welle.

Dieser Mechanismus wurde eingebaut in ein Computermodell der elektrischen Herzaktivität, das ein wahrheitsgetreues EKG mit 12 Ableitungen aussendet. Es zeigt sich, dass das Ansteigen der R-Zackenamplitude und der Kammeraktivierungszeit, die Abflachung und/oder die Polaritätsänderung der T-Welle bei Hypertrophie bedingt sind durch ein Anwachsen der Myokardzellgrösse, und dass die S-T-Veränderungen der akuten Ischämie bewirkt werden durch den Grenzflächeneffekt zwischen normalen und ischämischen Zellen. Für eine Läsion gegebener Grösse ist die S-T-Veränderung linear proportional zum Schweregrad, das heisst, zur Verminderung der elektrischen Aktivität der ischämischen Zellen. Bei gegebener Aktivitätsverminderung ist die S-T-Veränderung ein Mass für die Oberflächengrösse, nicht aber für das Volumen des ischämischen Gewebes. Somit besteht bei der akuten Ischämie keine zwangsläufige Korrelation zwischen volumenerfassenden Untersuchungen (wie die Serumenzymwerte bei der Nekrose) und S-T-Veränderungen.

Résumé

L'auteur décrit le mécanisme qui doit expliquer les tracés électrocardiographiques de l'hypertrophie cellulaire et de l'ischémie aiguë. Ce mécanisme prend naissance dans les cellules voisines ayant des potentiels d'action différents et se nomme effet de contiguité (contiguity effect). Cet effet de contiguité des

«couches Durrer» – qui sont définies – est la cause de l'inversion des ondes T dans l'hypertrophie, il est aussi responsable de la polarisation des ondes T normales.

Ce mécanisme a été incorporé dans un modèle mathématique de l'activité cardiaque, capable d'émettre un ECG de haute fidélité avec 12 dérivations. Il s'est avéré que l'augmentation d'amplitude de l'onde R et le temps d'activation des cavités cardiaques, ainsi que l'aplatissement et/ou l'inversion de la polarisation des ondes T dans l'hypertrophie sont dus à l'augmentation de grosseur de la cellule myocardique, et que les modifications de S-T dans l'ischémie aiguë sont provoquées par l'effet de contiguité entre des cellules normales et des cellules ischémiques. Dans une lésion de grandeur donnée les modifications S-T sont linéairement proportionelles à son importance, c'est-à-dire à la diminution de l'activité électrique des cellules ischémiques. Pour une diminution donnée de l'activité électrique, l'altération de S-T donne une mesure de la surface touchée, et non du volume du tissu ischémique. Il n'y a ainsi dans l'ischémie aiguë pas nécessairement de corrélation entre les modifications de S-T et les examens révélant le volume des lésions (comme les valeurs des enzymes sériques dans la nécrose).

Riassunto

Si descrive un meccanismo che spiega le manifestazioni elettrocardiografiche dell'ipertrofia cellulare e dell'ischemia acuta. Tale meccanismo che si origina in cellule vicine, aventi potenziali d'azione diversi, è stato definito «effetto di contiguità». Questo effetto di «strati Durrer» adiacenti (come vengono definiti nel testo) è all'origine delle alterazioni dell'onda T nei casi di ipertrofia ed è pure responsabile della polarità dell'onda T normale. Questo fenomeno è stato ricostituito per mezzo di un modello matematico dell'attività elettrica cardiaca, che è in grado di riprodurre elettrocardiogrammi a 12 derivazioni con estrema fedeltà. Si è cosi dimostrato che l'aumento dell'ampiezza delle onde R e del tempo d'attivazione ventricolare e l'appiattimento e/oppure l'inversione della polarità delle onde T nell'ipertrofia sono dovute ad un aumento delle dimensioni delle cellule miocardiche e che le variazioni del segmento ST nell'ischemia acuta sono dovute ad un «effetto di contiguità» tra cellule normali e cellule ischemiche. Per una lesione di dimensioni definite, le variazioni del segmento ST sono linearmente proporzionali alla sua «gravità»; cioè la riduzione dell'attività elettrica delle cellule ischemiche e, per una lesione di gravità definita, l'alterazione del segmento ST dà la misura dell'area del tessuto ischemico e non del suo volume. Di conseguenza non esiste necessariamente una correlazione diretta tra i parametri che misurano il volume del miocardio leso (quali le modificazioni degli enzimi del siero nei casi di necrosi) e le variazioni del segmento ST nell'ischemia acuta.

1. Thiry, P. and Rosenberg, R. M.: On electrophysiological activity of the normal heart, J. Frankl. Inst. (Mathematical Models of Biological Systems), *297*, 377–396, 1974.
2. Plonsey, R.: Bioelectric Phenomena, McGraw-Hill Book Company, New York, 1969, 228–288.
3. Durrer, D., van Dam, R. Th., Freud, G. E., Janse, M. J., Meijler, F. L. and Arzbaecher, R. C.: Total excitation of the isolated human heart, Circulation, *41*, 899–912, 1970.
4. Scher, A. M.: Excitation of the heart: A progress report *in* Advances in Electrocardiography: 61–71, Grune and Stratton, Inc., New York, 1972.
5. Selvester, R. H., Kalaba, R., Collier, C. R., Bellman, R. and Kagiwada, H.: A digital computer model of the vectorcardiogram with distance and boundary effects: Simulated myocardial infarction, Am. Heart J., *74*, 792–808, 1967.
6. Selvester, R. H., Solomon, J. C. and Gillespie, T. L.: Digital computer model of a total body electrocardiographic surface map: An adult male-torso simulation with lungs, Circulation, *38*, 684–690, 1968.
7. Selvester, R. H., Rubin H. B. and Ellis, E. J.: Vectorcardiographic and electrocardiographic estimate of myocardial damage, Circulation, *40*, Suppl. III: 182, 1969.
8. Selvester, R. H., Wagner, J. O. and Rubin, H. B.: Quantitation of myocardial infarct size and location by electrocardiogram and vectorcardiogram, *in* Quantitation in Cardiology: 31–44, The William and Wilkins Company, Baltimore, 1972.
9. van Dam, R. Th. and Durrer, D.: Experimental study on the intramural distribution of the excitability cycle and on the form of the epicardial T-wave in the dog heart in situ, Am. Heart J., *61*, 537–542, 1961.
10. Burgess, M. J., Green, L. S., Millar, K., Wyatt, R. and Abildskov, J. A.: The sequences of normal ventricular recovery, Am. Heart J., *84*, 660–669, 1972.
11. Wilson, F. N., MacLeod, A. G., Barker, P. S. and Johnston, F. D.: The determination and significance of the areas of ventricular deflections of the electrocardiogram, Am. Heart J., *10*, 46–61, 1934.
12. Harumi, K., Burgess, M. J. and Abildskov, J. A.: A theoretical model of the T-wave, Circulation, *34*, 659–668, 1966.
13. Burgess, M. J., Harumi, K. and Abildskov, J. A.: Application of a theoretic model to experimentally induced T-wave abnormalities, Circulation, *34*, 669–678, 1966.
14. Burgess, M. J.: Physiological basis of the T-wave *in* Advances in Electrocardiography: 367–375, Grune and Stratton, Inc., New York, 1972.
15. Thiry, P. S., Rosenberg, R. M. and Abbott, J. A.: A mechanism for the electrocardiogram response to left ventricular hypertrophy and acute ischemia, Circulation Res., *36*, 92–104, 1975.
16. Gelernter, H. L. and Swihart, J. C.: A mathematical physical model of the genesis of the electrocardiogram, Biophys. J., *4*, 285–301, 1964.
17. Scher, A. M., Ohm, W. W., Kerrick, W. G. L., Lewis, S. M. and Young, A. C.: Effects of body surface boundary and of tissue inhomogeneity on the electrocardiogram of the dog, Circulation Res., *29*, 600–609, 1971.
18. Geselowitz, D. B.: Electrical and magnetic field of the heart, Ann. Rev. Biophys., *2*, 37–64, 1973.
19. Geselowitz, D. B.: Model studies of electric and magnetic fields of the heart, J. Frankl. Inst., *296*, 379–391, 1973.
20. Karsner, H. T., Saphir, O. and Todd, T. N.: The state of the cardiac muscle in hypertrophy and atrophy, Am. J. Path., *1*, 351–371, 1925.
21. Lowe, T. E. and Bate, E. W.: The diameter of cardiac muscle fibers; a study of the diameter of muscle fibers in the left ventricle in normal hearts and in the left ventricular enlargement of simple hypertension, Med. J. Aust., *1*, 467–469; hyperplasia of cardiac muscle fibers, *ibid:* 618–620, 1948.

22. Uhley, H. N.: Electrophysiologic studies of left ventricular hypertrophy in rats, Circulation, *18*, 790, 1958.
23. Goldman, M. J.: Principles of Clinical Electrocardiography, Lange Medical Publications, Los Altos, Ca., 1973.
24. Prinzmetal, M., Ishikawa, K., Nakashima, M., Oishi, H., Ozkan, E., Wakayama, J. and Baines, J. M.: Correlation between intracellular and surface electrocardiograms in acute myocardial ischemia, Electrocardiol., *1*, 161–166, 1968.
25. Samson, W. E. and Scher, A. M.: Mechanism of S-T segment alteration during acute myocardial injury, Circulation Res., *8*, 780–787, 1960.

Address of author: Prof. Dr. R. M. Rosenberg, Department of Mechanical Engineering, University of California, Berkeley, Cal. 94720, U.S.A.